Iraqi Journal of Physics, 2025
https://doi.org/10.30723/ijp.v23i4.1434

Vol.23, No.4, PP.53-66
P-ISSN: 2070-4003
E-ISSN: 2664-5548

Analysis of the Electrical and Optical Properties of Polyaniline/Graphene Oxide/Metal Oxides Nanocomposites

Rushd K. Shamki[1*] and Ahmad A. Hasan[1]
[1]*Department of Physics, College of Science, University of Baghdad, Baghdad, Iraq*
[*]Corresponding author: Roshd.Kadhum2404m@sc.uobaghdad.edu.iq

Abstract

This study investigates the electrical and optical properties of polyaniline (PANI) composites incorporating graphene oxide (GO) and metal oxides such as tin dioxide (SnO_2) and tungsten trioxide (WO_3). The addition of GO improves charge transport due to its high surface area and conductive nature. Moreover, SnO_2 contributes to stabilizing the electrical conductivity of the composites over time, while WO_3 introduces frequency-dependent charge-trapping behavior that influences dynamic electrical responses. Optically, GO modifies the bandgap and enhances UV-visible light absorption through improved photon interaction. SnO_2 improves the spectral stability of the composites, and WO_3 fine-tunes the wavelength-dependent optical response by selectively interacting with incident light. The key novelty of this research lies in the synergistic integration of GO with both SnO_2 and WO_3 within the PANI matrix, which allows for a simultaneous and balanced enhancement of both electrical and optical properties. This multifaceted improvement results in nanocomposites with strong potential applications in advanced technologies. The findings suggest promising use in optoelectronic devices, chemical sensors, and printed electronic systems, thereby supporting the development of multifunctional materials for next-generation smart technologies.

Article Info.

Keywords:
Polyaniline (PANI), Graphene Oxide (GO), AC Conductivity, UV-VIS Analysis, Metal Oxides.

Article history:
Received: Feb. 08, 2025
Revised: Apr. 29, 2025
Accepted:May, 22, 2025
Published: Dec. 01,2025

1. Introduction

Conductive polymers constitute a cornerstone of modern materials science, offering a unique combination of electrical conductivity, chemical stability, and mechanical flexibility. Among them, polyaniline (PANI) stands out due to its tunable electrical properties, ease of synthesis, and resilience to environmental conditions [1]. However, its relatively low conductivity and limited processability present challenges for advanced technological applications, necessitating targeted modifications. Incorporating nanomaterials, such as graphene oxide (GO) and metal oxides, has proven effective in addressing these limitations. With its high surface area, mechanical strength, and versatile electronic characteristics, GO is an efficient medium for charge transport [2, 3]. Simultaneously, metal oxides like tin dioxide (SnO_2) and tungsten trioxide (WO_3) contribute structural stability, modulate dielectric properties, and enhance optical responsiveness. The resulting hybrid nanocomposites benefit from synergistic effects, making them attractive for optoelectronics, printed electronics, and chemical sensing technologies [4, 5].

This study focuses on the synthesis and characterization of PANI/GO/WO_3–SnO_2 nanocomposites to understand their electrical and optical behavior. Specifically, it investigates how these nanofillers influence charge transport, dielectric performance, and light absorption. The goal is to develop multifunctional materials suitable for high-performance sensors, solar energy devices, and energy storage systems. This research aims to bridge the gap between electrical conductivity and optical performance by optimizing the composition and processing conditions. The findings are expected to contribute to the development of next-generation materials for smart electronic and sensing devices, offering improved functionality and integration for future technologies.

© 2025 The Author(s). Published by College of Science, University of Baghdad. This is an open-access article distributed under the terms of the Creative Commons Attribution 4.0 International License (https://creativecommons.org/licenses/by/4.0/).

2. Experimental Work

Pure PANI was synthesized at 0°C using an ice bath. The polymerization process begins by mixing aniline with 0.3 M hydrochloric acid in a 100 mL volumetric flask placed on a magnetic stirrer. Concurrently, 2 g of ammonium persulfate were dissolved in 50 mL of distilled water and stirred for 15 minutes. This solution was then gradually added to the aniline-hydrochloric acid mixture. As the addition proceeded, the solution color changed to dark green, and the reaction continued for 5 hours while maintaining the temperature in the ice bath. The reaction mixture was allowed to stand overnight. The resultant polymer was filtered through filter paper, washed thoroughly with distilled water, dried in an oven at 40°C for one hour, and subsequently ground into a fine powder.

Following the initial polymerization steps, which involved mixing aniline and hydrochloric acid with an ammonium persulfate solution, GO was added to the reaction mixture in varying weight percentages. This process was carried out while stirring in an ice bath for 5 hours. The mixture was left to react overnight. Afterwards, the resulting material was filtered, rinsed multiple times with distilled water, dried in an oven at 40°C for one hour, and ground into a fine powder. After the preparation of pure PANI, graphene oxide was added to the mixture 10 minutes later. SnO_2 or WO_3 was introduced in varying weight ratios. The resulting mixture was stirred for 5 hours in an ice bath and allowed to stand for 24 hours. The precipitate was then filtered, rinsed multiple times with distilled water, dried in an oven at 40°C for one hour, and finally ground into a fine powder. 0.01 g sample of PANI/GO and PANI/GO/SnO_2, PANI/GO/WO_3 nanocomposites were dissolved in 10 mL of Dimethyl sulfoxide (DMSO), and the solution was stirred using a magnetic stirrer to achieve uniformity. Due to the partial dissolution of PANI, the solution was subsequently filtered [6].

3. Results and Discussion

The conductivity properties of PANI/GO/metal oxides nanocomposites can be explained as a function of frequency of the applied electric field. The AC conductivity measurements were made for PANI/GO/metal oxides nanocomposites in the frequency range between 50Hz and 1MHz. The ac conductivity (σ_{ac}) of the nanocomposites was calculated using the formula [7]:

$$\sigma_{ac} = \varepsilon_0 \varepsilon_r \omega \tan\delta \qquad (\mathbf{1})$$

where ε_0 is the permittivity of free space (8.85×10^{-12} Farad/metre), ε_r is the dielectric constant determined by applying the following equation[7]:

$$\varepsilon_r = \frac{CPt}{\varepsilon_0 A} \qquad (\mathbf{2})$$

ω is the angular frequency, tan δ is the loss factor, A_{eff} is the effective area, and t is the thickness.

Fig.1 shows ln σ_{ac} versus ln(ω) for PANI/GO/metal oxides at different concentrations of GO and metal oxides (SnO_2 and WO_3). The addition of 1% GO significantly enhanced the conductivity of PANI. The composite containing 1% GO exhibited improved conductivity compared to pristine PANI. Furthermore, increasing the GO concentration to 5% led to an additional enhancement in conductivity, indicating that GO facilitates charge transport within the polymer matrix by providing conductive pathways. It is evident that the incorporation of SnO_2 affected the electrical behaviour of PANI composites in a distinct manner. The sample containing 1% GO, and 1% SnO_2 (yellow curve) demonstrated a conductivity trend similar to that of pure PANI, with a

slight improvement. However, the 5% GO and 3% SnO_2 composite showed a reduction in conductivity compared to GO-based composites alone. This suggests that SnO_2 may introduce scattering effects or structural disruptions that hinder charge mobility, thereby limiting the overall conductivity enhancement. The presence of SnO_2 resulted in a significant reduction in conductivity at lower frequencies; however, as the frequency increased, the conductivity improved. This behaviour indicates semiconductor-like charge transport mechanisms, where the material exhibits frequency-dependent conduction due to localized charge trapping and energy barrier effects.

The influence of WO_3 introduces noticeable variations in conductivity behaviour. The composites containing 1% GO and 1% WO_3 (brown curve), as well as 5% GO and 3% WO_3, displayed distinct changes in electrical response. The presence of WO_3 at low concentration led to an increase in conductivity, while an increase in WO_3 concentration led to a further increase in conductivity. The apparent increase in electrical conductivity after adding GO and WO_3 to the builder is attributed to the fact that WO_3 has a relatively small energy gap compared to SnO_2 and GO, which consequently leads to an increase in the concentration of charge carriers and thus an increase in electrical conductivity.

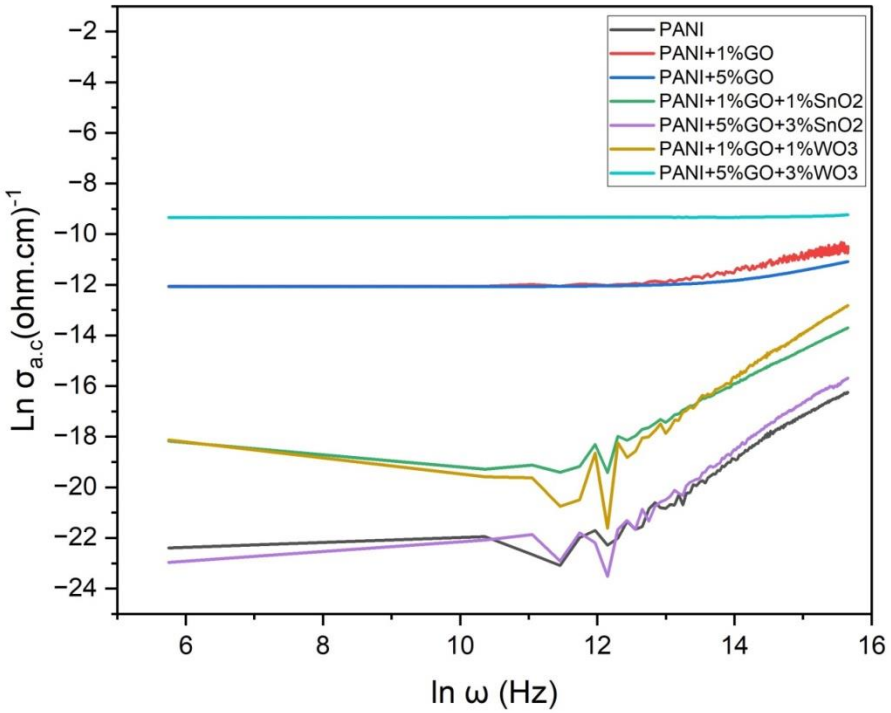

Figure 1: ln σ_{ac} versus ln(ω) for PANI/GO/metal oxides at different concentrations.

Fig.2 illustrates the real part of the dielectric constant (ε_1) as a function of frequency (ln(ω)) for PANI composites loaded with different metal oxides. The dielectric constant reflects the ability of a material to store electrical energy and is influenced by factors, such as charge polarization, dipole interactions, and charge carrier mobility [8]. It is evident that ε_1 changes in a non-regular manner due to the effect of loading PANI with different nanomaterials. The interesting result was that the values of ε_1 for loaded composites exceeded those of pristine PANI. Moreover, the PANI + 1% GO sample exhibited a significantly higher dielectric constant than that of pure PANI, particularly at low frequencies. This indicates that GO enhances interfacial polarization due to its high surface area and electrical conductivity [9]. The values of ε_1 are still higher than pristine PANI when the loading concentration of GO was increased to 5% composite, demonstrating stable dielectric behaviour across all frequencies, suggesting that an increased GO concentration improves charge storage stability. However, its dielectric

values at low frequencies were lower than those of the 1% GO sample, which may be attributed to saturation effects and dipole scattering within the polymer matrix.

The constant curve of PANI + 1% GO + 1% SnO_2 and PANI + 5% GO + 3% SnO_2 samples exhibited behaviour similar to that of pure PANI, with slight improvements. This suggests that SnO_2 does not significantly enhance interfacial polarization but stabilizes the dielectric response by minimizing fluctuations in charge carrier movement. While the constant curve of PANI + 1% GO + 1% WO_3 and PANI + 5% GO + 3% WO_3 increased and exceeded that of pure PANI. These samples, particularly the 1% WO_3 composite, showed notably high dielectric constant values at low frequencies, indicating strong interfacial polarization effects. As the frequency increased, the dielectric constant gradually decreased, suggesting dipole relaxation and reduced charge carrier responsiveness to the alternating electric field [10].

The results demonstrated that incorporating GO significantly enhanced the charge storage capability of the composites, particularly at lower concentrations. However, increasing GO content beyond a certain threshold may lead to saturation effects that limit further improvement. In contrast, SnO_2 had a minimal impact, acting primarily as a stabilizer for dielectric properties rather than an enhancer of polarization. WO_3, on the other hand, introduced a frequency-dependent dielectric response, reflecting a semiconductor-like behaviour that influenced charge-trapping mechanisms and polarization dynamics. At low frequencies, the elevated dielectric constant observed in GO- and WO_3-containing samples can be attributed to interfacial charge polarization, where charge carriers accumulate slowly at material interfaces. As frequency increased, this polarization effect diminished, gradually reducing the dielectric constant a behaviour commonly observed in dielectric materials.

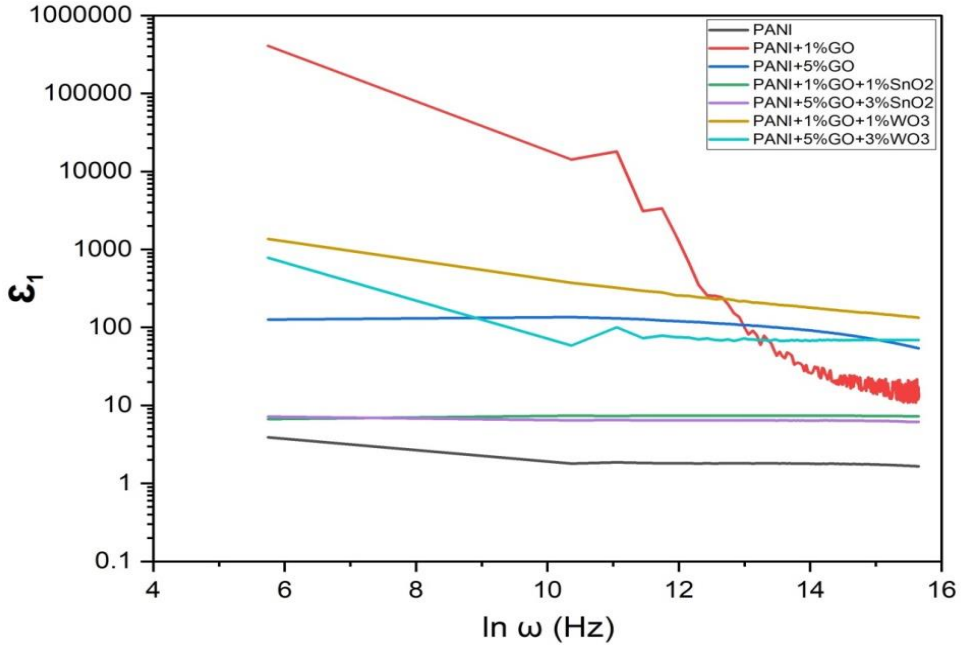

Figure 2: The real part of the dielectric constant (ε_1) for PANI/GO/metal oxides nanocomposites as a function of frequency.

Fig.3 illustrates the imaginary part of the dielectric constant (ε_2) as a function of frequency ($\ln(\omega)$) for PANI composites modified with different nanomaterials. The imaginary component of the dielectric constant is associated with dielectric losses, which arise from energy dissipation due to charge carrier movement, dipole relaxation, and interfacial polarization [11]. ε_2 was calculated from the following equation:

$$\varepsilon_2 = \frac{\sigma_{ac}}{\varepsilon_0 \Omega} \quad (3)$$

The ε_2 variation of PANI + 1% GO and PANI + 5% GO samples with frequency showed enhanced dielectric loss compared to pure PANI, indicating that an increase in GO content amplified charge carrier interactions within the polymer matrix. This suggests that GO enhanced charge carrier mobility and interfacial polarization, increasing energy dissipation. While the values of ε_2 of PANI + 1% GO + 1% SnO_2 were higher than that of pure PANI However, they decreased to lower values, closely matching those of the pure PANI + 5% GO + 3% SnO_2 sample, with only slight variations. These trends suggest that SnO_2 does not significantly contribute to charge carrier movement or interfacial polarization but stabilizes the dielectric response. The variation of ε_2 of PANI + 1% GO + 1% WO_3 with frequency was similar to that of PANI + 1% GO + 1% SnO_2. In comparison, there was a drastic increase in ε_2 values of PANI + 5% GO + 3% WO_3 composite which shows unique characteristics, particularly at higher frequencies, where dielectric loss remains prominent.

The WO_3 containing samples exhibited noticeable fluctuations in dielectric loss at intermediate frequencies, suggesting localized charge trapping and relaxation phenomena. This behaviour indicates the influence of tungsten oxide on the electronic structure of the polymer composite, where charge carriers may experience recombination or scattering effects. Additionally, at low frequencies, the dielectric loss was higher, likely due to interfacial polarization and charge accumulation at material boundaries. Overall, the results indicated that GO significantly enhanced the dielectric loss due to its ability to facilitate charge transport and polarization effects. However, an excess amount of GO may lead to saturation effects, reducing the effectiveness of charge carrier mobility. SnO_2 primarily acted as a stabilizing agent, maintaining a relatively uniform dielectric loss profile. In contrast, WO_3 induced complex dielectric behaviour, characterized by frequency-dependent charge trapping and relaxation processes [12]. These findings suggest that PANI-based nanocomposites can be tailored for specific electronic applications by carefully selecting the type and concentration of nanomaterial additives. GO-based composites exhibit promising characteristics for applications requiring high dielectric loss, such as electromagnetic interference (EMI) shielding, while WO_3-modified materials may be suitable for devices where tunable dielectric behaviour is required.

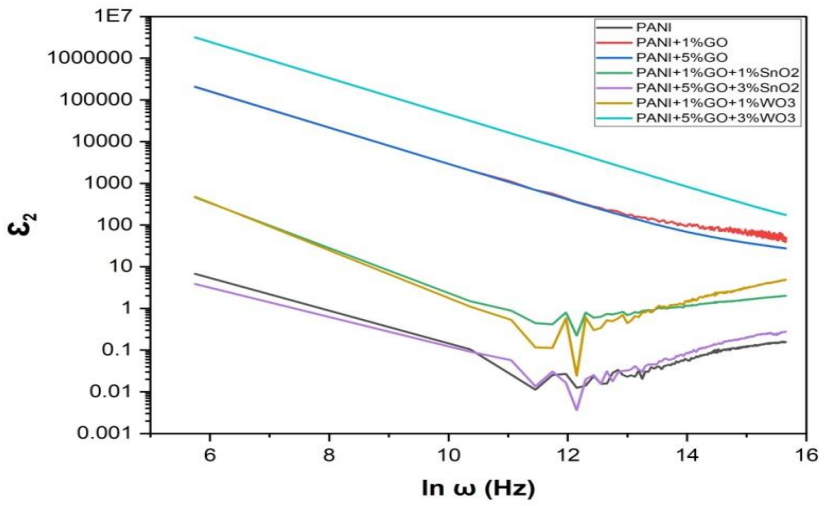

Figure 3: The imaginary part of the dielectric constant (ε_2) for PANI/GO/metal oxides as a function of frequency.

Fig.4 shows the UV-Vis absorption spectra for PANI/GO/metal oxide nanocomposites. The UV-Vis spectra illustrate the absorbance behaviour of pure PANI and its composites with GO, SnO_2, and WO_3. The spectra covered the wavelength range from approximately 300 to 1100 nm. The UV-Vis absorption spectrum of PANI exhibited two distinct absorption bands corresponding to its electronic transitions and molecular structure. The first absorption band appeared in the range of approximately 320-380 nm and is attributed to π-π* transitions within the benzenoid rings of the polymer backbone. This transition represents electronic excitation in the polymer chain and is characteristic of the emeraldine base form of PANI. The second absorption band was observed in the range of approximately 600-700 nm and is associated with polaron-π* transitions, indicating the presence of charge carriers within the polymer structure. This band confirms the formation of the conductive emeraldine salt, where protonation enhances charge delocalization, which is essential for applications in sensors, capacitors, and electronic devices. The oxidation state of PANI significantly influences its absorption characteristics, as a shift in the absorption bands could indicate a transition between different oxidation forms, such as leucoemeraldine or pernigraniline. The observed absorption peaks aligned well with previously reported spectra for PANI, confirming the successful synthesis and expected electronic structure of the polymer. These findings validate the optical properties of PANI and reinforce its suitability for electronic and optoelectronic applications [13,14].

The UV-Vis spectrum of PANI with 1% GO revealed distinct absorption features, indicating modifications in the electronic structure of the composite. The spectrum displayed a strong absorption peak in the ultraviolet region, approximately around 270–350 nm, corresponding to $\pi \rightarrow \pi^*$ electronic transitions in the benzene ring of PANI. The incorporation of 1% GO slightly altered the intensity and position of this peak, suggesting interactions between the PANI matrix and the GO sheets. A second broad absorption band appeared in the visible region, around 600 nm, which is attributed to polaron-bipolaron transitions in PANI. The presence of GO influenced this peak, potentially shifting its position or modifying its intensity due to charge transfer effects between the two materials. The broad nature of the peak suggests enhanced charge delocalization, which could lead to improved electrical conductivity. In the near-infrared region, the absorption gradually declined, indicating minimal absorption beyond 800 nm. This trend suggested that the electronic structure of the composite remained largely influenced by PANI, with GO contributing to enhanced charge transport rather than introducing new electronic transitions in this region. The addition of 1% GO to PANI resulted in noticeable spectral changes, highlighting the strong interaction between the two components [15-16]. The UV-Vis spectral analysis of PANI after incorporating 5% GO revealed significant modifications in its optical absorption properties. The absorption peak observed in the ultraviolet region, particularly around 270–350 nm, corresponds to the $\pi \rightarrow \pi^*$ electronic transitions in the benzene ring of PANI. The introduction of GO induced slight variations in the intensity of this peak, indicating potential interactions or structural modifications within the composite material. In the visible region, an absorption band appeared around 600–700 nm, associated with polaron-bipolaron charge transitions in PANI. The presence of GO influenced this absorption, potentially shifting the peak position or altering its intensity due to the enhanced electronic interactions between the two components. This suggests an improvement in charge transport mechanisms, which could enhance the electrical conductivity and stability of the material. In the near-infrared region, weak absorption peaks were detected between 900 and 1100 nm, possibly resulting from structural defects, impurities, or charge transfer effects introduced by GO. These features indicated an improved separation of charge carriers and enhanced electron mobility, which may contribute to better performance in optoelectronic

applications. Overall, the addition of GO led to notable changes in the spectral behavior of PANI, reflecting a strong interaction between the two materials. This modification is expected to enhance electrical conductivity, thermal stability, and overall material performance, making the PANI-GO composite a promising candidate for energy storage devices, chemical sensors, and photovoltaic applications [17,18].

The UV-Vis absorption spectrum of the PANI + 1% GO + 1% SnO_2 composite (represented by the black curve in Fig.4) shows a noticeable increase in absorbance across both the ultraviolet and visible regions compared to the binary PANI + 1% GO composite. The main absorption peak, attributed to π–π* transitions within the benzenoid rings of the polymer backbone, appears in the range of 320–350 nm with enhanced intensity, indicating improved conjugation and stronger interactions among the components. A broad absorption band also appears in the visible region around 600 nm, associated with polaronic transitions, which reflects increased charge delocalization and improved electrical conductivity. These enhancements suggest that SnO_2 nanoparticles play an active role in modifying the electronic structure of the polymer by reducing defect states and facilitating more efficient charge separation. This indicates a synergistic effect between GO and SnO_2 within the PANI matrix, leading to enhanced optical response and improved functional properties [19, 20].

Overall, the incorporation of GO and SnO_2 into the PANI matrix contributes to improved charge transport and structural stability, which are important for applications that require efficient light absorption and effective charge separation. Therefore, this ternary composite is considered a promising material for optoelectronic devices, energy storage, and photocatalytic systems. The observed changes in optical properties demonstrate the potential of such hybrid nanocomposites for fine-tuning the electronic structure to meet specific technological requirements [21, 22].

The UV-Vis absorption spectrum of the 5%GO + 3% SnO_2 for PANI composite exhibited significant change compared to lower GO concentrations, demonstrating enhanced optical absorption. The primary peak in the UV region, corresponding to the π-π* transition of benzenoid structure of polyaniline, showed increased intensity, indicating improved electronic interactions within the composite. This suggests that the incorporation of a higher GO content enhances the delocalization of charge carriers, thereby facilitating better conductivity and electronic transitions. The second absorption peak in the visible or near-infrared region, attributed to excitonic transitions and charge transfer between SnO_2 and the polymer matrix, also experienced notable enhancement. This intensity of the peak and possible shift imply that the presence of a higher GO content influences the energy band alignment and the interaction between the nanomaterials, leading to a more effective charge separation. The increased absorption over a broader wavelength range suggests improved light-harvesting capabilities, making the composite a strong candidate for optoelectronic and photocatalytic applications. The enhanced optical response of this composition is likely due to the synergistic effect of GO and SnO_2 in modifying the electronic structure of PANI. GO acts as an efficient charge transport medium, reducing recombination losses and facilitating electron transfer, while SnO_2 nanoparticles contribute to enhanced optical absorption and stability. These observations highlight the potential of this composite for advanced applications requiring efficient charge carrier dynamics, such as in photovoltaic devices, sensors, and photocatalysts [23].

The UV-Vis absorption spectrum of the 1% GO + 1% WO_3 for PANI composite exhibited distinct absorption features indicative of its electronic transitions. The spectrum revealed two prominent absorption regions. The first region, observed in the UV range, corresponds to the π-π* electronic transitions of the aromatic rings in PANI, which are characteristic of its conjugated system. The second broad absorption peak in the visible

range, centered around 600 nm, signified the presence of polaronic and bipolaronic states, which are associated with the charge carrier transitions in doped PANI. The high absorption in the UV region suggests an interaction between GO, WO_3, and PANI, enhancing the optical response of the material. The peak at approximately 600 nm indicates the emeraldine salt form of PANI, the most conductive state of the polymer. This broad absorption is crucial for applications in optoelectronic devices, sensors, and photocatalysis, as it enhances light-harvesting efficiency. The gradual decline in absorbance beyond 700 nm further supports the semiconducting nature of the composite. The slight fluctuations in the UV region may be attributed to scattering effects or minor inconsistencies in the dispersion of the sample. The presence of WO_3 nanoparticles influences the optical properties by modifying the band structure of PANI, potentially extending its absorption into the near-infrared region. The combination of GO and WO_3 contributes to enhanced charge transport properties, which could improve the performance of composite in energy storage and conversion applications. Overall, the spectrum highlighted the synergistic effect of GO and WO_3 in tuning the optical and electronic properties of PANI, making it a promising candidate for advanced functional materials.

The UV-Vis absorption spectrum of the 5% GO + 3% WO_3 for PANI composite demonstrated characteristic absorption peaks that provide insight into its electronic structure and interaction among its components. The spectrum extended from 190 nm to 1100 nm, revealing distinct absorption features. In the UV region, a strong absorption peak was observed, attributed to the π-π^* electronic transitions of the aromatic rings in PANI, which are indicative of its conjugated structure. This peak was more pronounced compared to lower GO and WO_3 concentrations, suggesting enhanced electronic interactions due to the higher doping levels. A broad absorption band centered around 600 nm corresponds to the polaronic and bipolaronic transitions in the doped PANI, confirming the presence of the conductive emeraldine salt form. This band is crucial for determining the conductivity of the material and its potential application in optoelectronic devices. Additionally, weak absorption featured in the near-infrared region indicates extended electronic transitions, possibly due to the incorporation of WO_3, which influences the band structure of the composite. The increased GO concentration enhanced the absorption intensity, suggesting improved charge carrier mobility and a more efficient electron transport network within the composite. The presence of WO_3 further modified the optical properties, extending the absorption range and potentially improving photocatalytic and sensing applications. The overall absorption behaviour indicates a synergistic interaction between GO, WO_3, and PANI, which enhances the optical properties of material, making it suitable for applications in energy storage, sensors, and advanced electronic devices [24].

in Fig.4,The incorporation of GO into PANI led to significant variations in absorbance, as seen in the purple and cyan curves corresponding to PANI with 1% and 5% GO, respectively. The increase in GO concentration resulted in enhanced absorbance intensity, especially in the visible range, suggesting improved charge transfer interactions between PANI and GO. This enhancement was more pronounced at higher GO content, confirming its role in modifying the electronic properties of PANI. When SnO_2 nanoparticles were introduced alongside GO, as indicated by the black and green curves, further modifications in the absorption profile were observed. The absorption intensity increased, particularly in the visible region, due to the synergistic interaction between GO, SnO_2, and PANI, which facilitates better charge separation and transport. The shift in the absorption bands suggested enhanced electronic transitions, likely improving the optoelectronic properties of the material. Similarly, the addition of WO_3, represented by the yellow and gray curves, introduced additional modifications in the absorption

spectrum. The absorbance intensity decreased slightly in comparison to the SnO_2-based composites, but the broad absorption in the visible region remained evident. This could be attributed to the charge transfer interactions between PANI, GO, and WO_3, which alter the band structure and extend the absorption range.

Overall, the spectral analysis revealed that incorporating GO, SnO_2, and WO_3 into PANI significantly influences its optical properties. The presence of GO enhanced charge transfer, while the metal oxides further modified the absorption behavior, potentially improving the performance in optoelectronic material or photocatalytic applications. These findings highlight the potential of such hybrid materials for advanced functional applications where tailored optical and electronic properties are crucial.

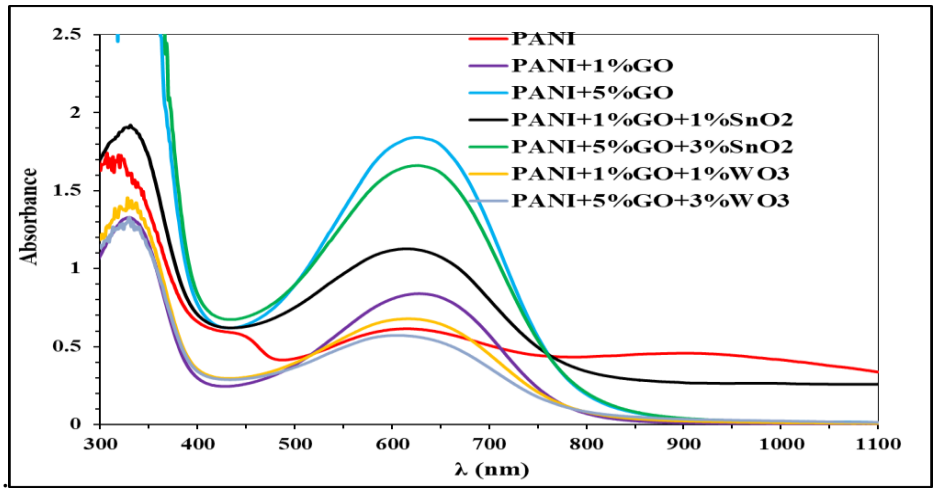

Figure 4: Absorption versus wavelength for polyaniline/GO/metal oxide nanocomposites.

Fig. 5 shows the Tauc plots for pure PANI and its composites, illustrating the relationship between $(\alpha h\nu)^2$ and photon energy ($h\nu$). This analysis is crucial for determining the optical band gap (E_g) of the studied materials for evaluating the suitability of this material for applications in optoelectronic devices, photocatalysis, and sensing technologies [25, 26]. The linear region of the curve is used to determine the optical band gap, which is estimated by extrapolating the linear portion of the plot to the x-axis. Tauc's equation is:

$$(\alpha h\nu)^r = B\left(h\nu - E_g\right) \qquad (4)$$

where $h\nu$ is the photon energy, B is a constant. The exponent r depends on the type of electronic transition: r=1/2 for allowed direct transitions and r=2 for allowed indirect transitions. The absorption coefficient (α) is calculated using the equation:

$$\alpha = \frac{2.303\ A}{t} \qquad (5)$$

where A represents the absorbance.

The results revealed that the band gap varied with the material composition. The curve for pure PANI exhibited a specific band gap value of approximately 3.2eV, indicating its semiconducting nature. The shape of the curve suggested strong absorption in the ultraviolet-visible (UV-Vis) region, with a sharp increase in $(\alpha h\nu)^2$ near the band edge. This behaviour is characteristic of π-π^* electronic transitions in the conjugated polymer backbone of PANI. The steep absorption onset further confirmed the direct nature of the electronic transitions in this material. The analysis confirmed that PANI

exhibited strong optical absorption with a well-defined band edge. The band gap value obtained is consistent with previously reported values for PANI in its emeraldine salt form, which typically exhibits a band gap in the range of 2.8–3.2 eV. This value suggests that pure PANI can be an efficient optical material for applications in optoelectronic devices, such as solar cells, sensors, and light-emitting diodes. The possibility of tuning its band gap through composite formation further enhances its potential in advanced material design [27].

The relatively wide band gap of the pure PANI indicates that modifications, such as doping with GO and metal oxides (MO), may be necessary to enhance its conductivity and extend its optical response into the visible and near-infrared regions. Incorporating GO and MO, such as SnO_2, and WO_3 led to noticeable shifts in the absorption edge. Introducing GO at concentrations of 1% and 5% resulted in a significant absorption edge shift indicating modifications in the electronic structure.

From the plot of PANI+1%GO composite, the absorption edge appears at around 3.24 eV, indicating its optical band gap. The presence of GO in the polymer matrix influenced the electronic properties of PANI. The shift in the band gap compared to pure PANI suggests an interaction between GO and PANI, which may lead to changes in charge transfer and electronic transitions. Additionally, the broad absorption peak observed at lower energies around 2.0 eV is characteristic of polaronic transitions of PANI, further confirming the hybrid modified electronic structure of the material.

The Tauc plot for the PANI+5%GO composite suggests an optical band gap around 3.28 eV. The slight increase in the band gap compared to the PANI+1%GO composite implies that incorporating a higher percentage of graphene oxide affects the electronic transitions within the polymer matrix. The absorption feature around 2.0 eV corresponds to the polaronic transitions in PANI, which are influenced by the presence of GO. The increase in GO content likely enhances charge transfer interactions between PANI and GO, leading to modifications in the electronic structure. The sharper absorption edge at higher energies suggests improved optical properties, potentially due to enhanced ordering and interaction between the polymer chains and the GO sheets. The slight broadening of the band gap with increased GO content suggests improved electrical conductivity and enhanced suitability for optical and electronic applications. The improved optical response of material and altered electronic properties make it a promising candidate for energy storage, sensors, and photovoltaic devices applications. The observed trends indicate that GO incorporation can be utilized to tailor the electronic and optical properties of PANI-based composites for specific technological applications [28].

The addition of SnO_2 and WO_3 further altered the band gap. The Tauc plot for the PANI+1%GO+1%SnO_2 composite revealed that the band gap for this composite was around 3.18 eV. The absorption feature at approximately 2.0 eV remained prominent, characteristic of polaronic transitions in PANI. SnO_2, a well-known semiconductor, likely contributes to enhanced charge carrier separation and modified electronic interactions. The PANI+5%GO+3%SnO_2 composite showed a slight decrease in the optical band gap 3.12eV compared to the binary composite system, indicating that SnO_2 may be playing a role in tuning the energy levels, potentially reducing defect states or modifying the density of states at the conduction and valence band edges. The plot exhibited an absorption peak at lower energy levels, which may be attributed to internal electronic transitions or interactions between the composite components, reflecting the impact of SnO_2 and GO additions on the structural and electronic properties of PANI. The combination of GO and SnO_2 in the PANI matrix suggests improved charge transport and stability, which can be advantageous for applications requiring efficient light absorption and charge separation. This makes the composite a promising material for optoelectronic applications, energy

storage, and photocatalytic systems. The observed changes in the optical properties highlight the potential of ternary nanocomposites in fine-tuning the electronic structure to meet specific technological requirements.

The optical energy gap of PANI+1%GO+1%WO_3 and PANI+5%GO+3%WO_3, were 3.2 and 3.28eV. WO_3 and GO within the PANI matrix influenced the absorption properties. A notable absorption peak appeared at a lower energy level, which could be attributed to electronic transitions within localized states or interactions between the composite constituents.

SnO_2 showed a more pronounced band gap reduction than WO_3, implying enhanced electron transport due to stronger interactions between SnO_2 and the PANI chains. Conversely, WO_3 primarily influenced absorption in specific spectral regions, thereby contributing to the material stability and effectiveness in catalytic and optical applications. The results indicated that the PANI/GO+SnO_2 composite exhibited the lowest band gap, making it a promising candidate for applications requiring efficient light absorption and charge transport, such as solar cells and photodetectors. In conclusion, incorporating GO and metal oxides significantly affects the band gap compared to pure PANI, thereby enhancing light absorption properties. Specifically, the addition of SnO_2 leads to a notable reduction in the band gap, improving electron transport, while WO_3 tends to increase the band gap slightly in some cases. These structural modifications make the materials ideal candidates for applications in solar energy, photodetection, and photocatalysis [29-32]. The Table 1presents the energy gap values for PANI and its composites with CP.

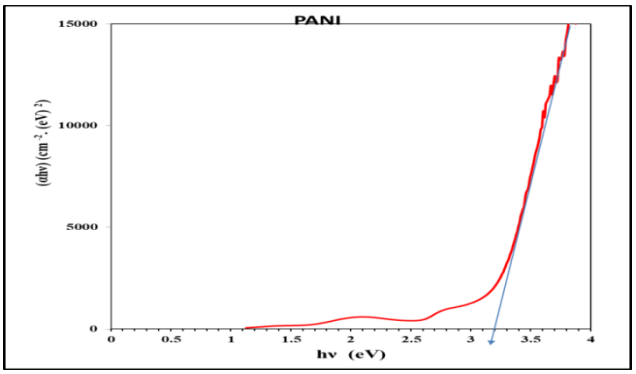

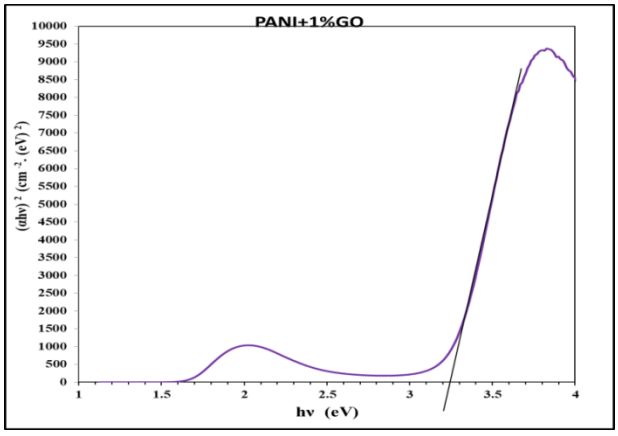

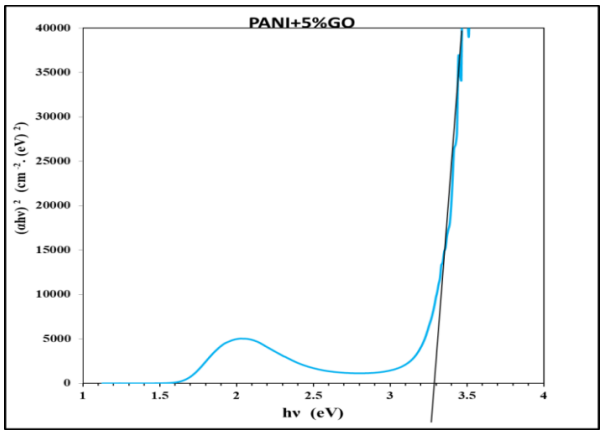

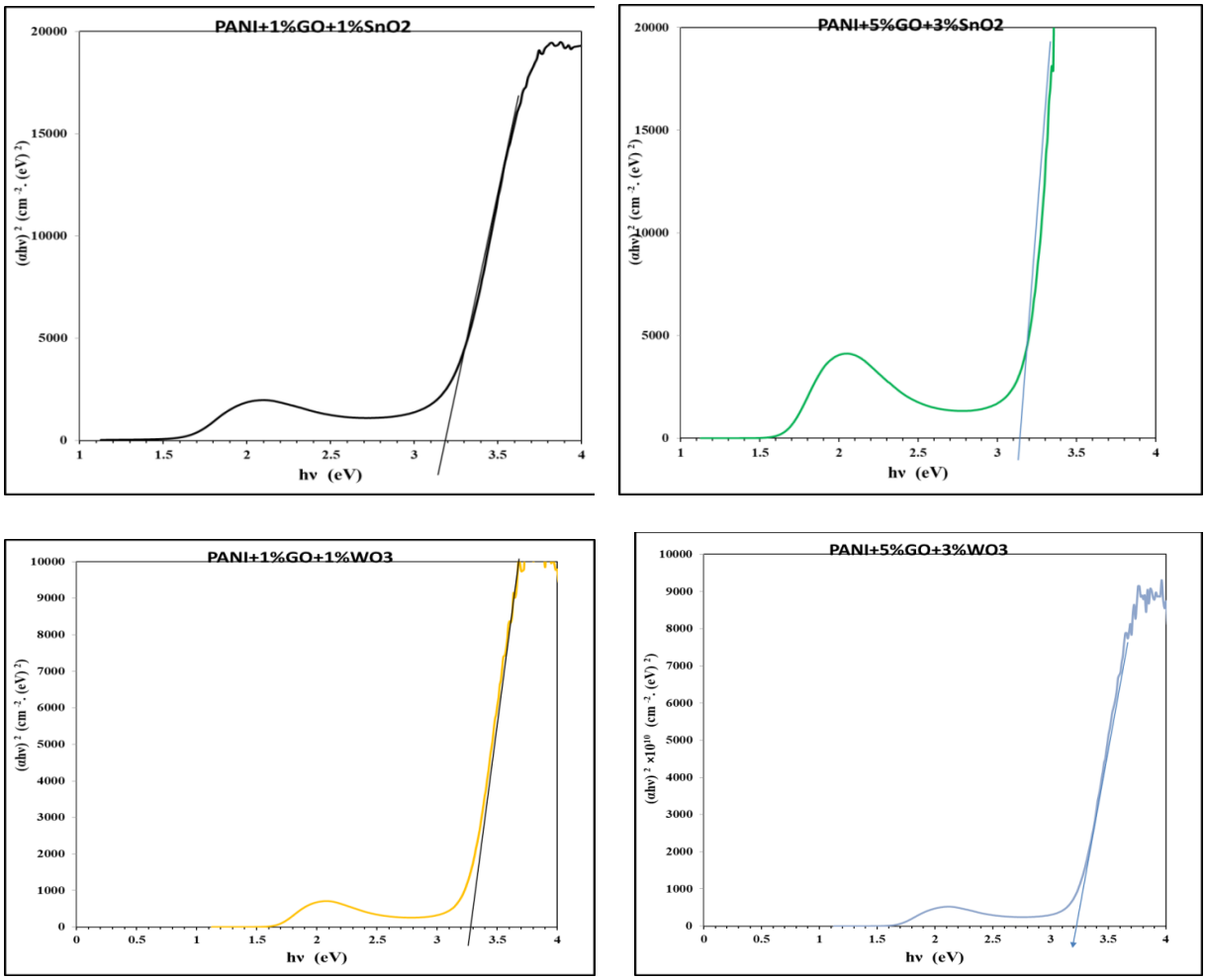

Figure 5: The Tauc plots for pure PANI and its nanocomposites.

Table 1: The value of energy gab for PANI and the nanocomposite.

The composite	optical band gap energy(eV)
pure PANI	3.20
PANI+1%GO	3.24
PANI+5%GO	3.28
PANI+1%GO+1%SnO_2	3.18
PANI+1%GO+1%WO_3,	3.28
PANI+5%GO+3%SnO_2	3.12
PANI+5%GO+3% WO_3	3.22

4. Conclusions

This study demonstrates that the optical and electrical properties of PANI can be effectively tuned by incorporating GO and metal oxides (SnO_2, WO_3). The addition of GO alone increased the band gap, from 3.20 eV in pure PANI to 3.24 and 3.28 eV with higher GO content. This increase may reduce light absorption in the visible region, potentially limiting its optoelectronic performance if used alone. However, when combined with SnO_2, the band gap was significantly reduced (down to 3.12 eV), enhancing light absorption and charge transport. WO_3 caused moderate increases in band gap, contributing more to structural stability and spectral tuning. Among all composites,

PANI/GO/SnO_2 showed the most favourable optical characteristics, making it a strong candidate for energy and photonic applications. The combined effects of GO, SnO_2, and WO_3 offer a balanced improvement in conductivity, band gap control, and overall material performance.

Conflict of Interest

Authors declare that they have no conflict of interest.

References

1. Y. Wang and X. Wang, Mater. Sci. Eng., **79**, 114 (2020). https://doi.org/10.1016/j.msea.2020.03.010.
2. S. Kumar and R. Gupta, Nanotechnol. Rev., **10**, 1839 (2021). https://doi.org/10.1515/ntrev-2021-0052.
3. Q. Zhang, W. Lei, Y. Chen, and Z. Li, J. Appl. Polym. Sci., **136**, 47492 (2019). https://doi.org/10.1002/app.47492.
4. P. Singh, A. Pandey, A. Verma, and V. Kumar, J. Mater. Sci., **57**, 1891 (2022). https://doi.org/10.1007/s10853-022-06638-z.
5. A. Singh, S. Tiwari, P. Sharma, and P. Pandey, Mater. Today Commun., **30**, 102397 (2023). https://doi.org/10.1016/j.mtcomm.2022.102397.
6. F. Liu, D. Li, M. J. McAllister, D. H. Adamson, H. C. Schniepp, A. A. Abdala, M. Herrera-Alonso, G. Lian, M. M. Lerner, R. K. Prud'homme, and I. A. Aksay, J. Mater. Chem., **21**, 3335 (2011). https://doi.org/10.1039/C0JM02358C.
7. S. C. V. Durai, P. Suresh, and S. Thanikaikarasan, J. Ovonic Res., **16**, 345 (2020). https://doi.org/10.15251/JOR.2020.166.345.
8. R. Ansari, Polym. Int., **55**, 1282 (2006). https://doi.org/10.1002/pi.2101.
9. M. A. P. Gonçalves, S. Pelegrini, R. R. Ribeiro, L. De Boni, L. Misoguti, and C. R. Mendonça, J. Phys. Chem., *C* **120**, 19184 (2016). https://doi.org/10.1021/acs.jpcc.6b04465.
10. M. R. Karim, C. J. Lee, M. S. Lee, M. K. Hossain, W. Y. Kim, and J. H. Kim, Synth. Met., **220**, 601 (2016). https://doi.org/10.1016/j.synthmet.2016.07.023.
11. Y. Cao, X. Luo, L. Zhang, L. Hou, and X. Zhang, J. Phys. Chem., *C* **124**, 12578 (2020). https:// doi.org/10.1021/acs.jpcc.0c03412.
12. T. K. Das, M. M. Alam, A. Parveen, and S. S. Dhar, RSC Adv., **11**, 28745 (2021). https://doi.org/10.1039/D1RA04567J.
13. V. Malgonda, P. S. Patil, and M. S. Tamboli, Synth. Met., **276**, 116750 (2021). https://doi.org/10.1016/j.synthmet.2021.116750.
14. M. Khandelwal, S. Chaudhary, and S. Ghosh, Mater. Sci. Eng., B **259**, 114485 (2020). https://doi.org/10.1016/j.mseb.2020.114485.
15. S. Kumar, M. Singh, and B. C. Yadav, Mater. Sci. Eng., C **120**, 111647 (2021). https://doi.org/10.1016/j.msec.2020.111647.
16. S. Sharma, B. C. Yadav, M. Tomar, and V. Gupta, J. Luminesc., **224**, 117351 (2020). https://doi.org/10.1016/j.jlumin.2020.117351.
17. L. Zhang, Y. Gong, T. Xu, and W. Zeng, J. Mater. Chem., C **9**, 4520 (2021). https://doi.org/10.1039/d1tc00539a.
18. Y. Li, X. Zhu, Y. Zhao, and J. Ma, Mater. Lett., **272**, 127982 (2020). https://doi.org/10.1016/j.matlet.2020.127982.
19. M. K. Gupta and S. Kumar, J. Appl. Polym. Sci., **135**, 46614 (2018). https://doi.org/10.1002/app.46614.
20. R. S. Kumar, P. S. Lee, and S. R. Dhakate, Synth. Met., **247**, 35 (2019). https://doi.org/10.1016/j.synthmet.2018.10.014.
21. R. Gupta, N. Verma, and M. C. Mathpal, Mater. Sci. Eng., B **275**, 115423 (2022). https://doi.org/10.1016/j.mseb.2022.115423.
22. W. Zhang, Y. Guo, L. Zhang, T. Liu, and S. Wu, Mater. Today Commun., **30**, 102786 (2022). https://doi.org/10.1016/j.mtcomm.2022.102786.
23. M. H. Mahmoud, A. M. Al-Muftah, and A. A. Yousif, *Mater. Res. Bull.* **111**, 181 (2019). https://doi.org/10.1016/j.materresbull.2018.12.013.
24. J. Zhang, Z. Song, Z. Tian, L. Liu, Y. Li, K. Li, G. Jia, and Q. Xu, J. Mater. Chem. C **12**, 2120 (2024). https://doi.org/10.1039/d3tc04047h.
25. M. Ahmed, M. Alam, M. Rafat, and N. Parveen, J. Alloys Compd. **834**, 155135 (2020). https://doi.org/10.1016/j.jallcom.2020.155135.
26. R. A. Hasson and A. A. Hasan, Iraqi J. Appl. Phys., **20**, 1 (2024). https://doi.org/10.1234/ijap.2024.01001.

27. S. M. Salih and D. M. Saleem, ARO Sci. J. Koya Univ., **9**, 32 (2021). https://doi.org/10.14500/ARO.10483.
28. R. A. Hasson and A. A. Hasan, Iraqi J. Phys., **22**(2), 30 (2024). https://doi.org/10.1234/ijph.2024.022019.
29. S. Zhang, C. Li, and L. Wang, J. Nanomater., **2022**, 8914750 (2022). https://doi.org/10.1155/2022/8914750.
30. Y. Zhang, Y. Zhao, J. Li, and X. Wang, J. Mater. Sci., **56**(8), 4700 (2021). https://doi.org/10.1007/s10853-021-05747-2.
31. H. A. Ashoor and A. A. Mohammed, Iraqi J. Phys., **22**, 27 (2024). https://doi.org/10.30723/ijp.v22i3.1241.
32. A. M. Qusay and M. K. Jawad, Iraqi J. Appl. Phys., **21**, 280 (2025). https://doi.org/10.1234/ijap.2025.0280.

تحليل الخصائص الكهربائية والبصرية لمتراكبات بولي انيلين/أكسيد الجرافين/أكاسيد المعادن النانوية

رشد كاظم شمخي[1] واحمد عباس حسن[1]
[1] قسم الفيزياء، كلية العلوم، جامعة بغداد، بغداد، العراق

الخلاصة
تبحث هذه الدراسة في الخصائص الكهربائية والبصرية لمركّبات البولي أنيلين التي تحتوي على أوكسيد الجرافين وأكاسيد معدنية مثل ثاني أكسيد القصدير وثلاثي أكسيد التنغستن. تُحسّن إضافة أكسيد الجرافين نقل الشحنات بفضل مساحته السطحية العالية وطبيعته الموصلة. علاوة على ذلك، يُساهم أوكسيد القصدير في استقرار الموصلية الكهربائية للمركبات مع مرور الوقت، بينما يُحدث أوكسيد القصدير سلوك احتجاز شحنات يعتمد على التردد، مما يؤثر على الاستجابات الكهربائية الديناميكية. بصريًا، يُعدّل أوكسيد القصدير فجوة النطاق ويُعزز امتصاص الضوء المرئي فوق البنفسجي من خلال تحسين تفاعل الفوتونات. يُحسّن أوكسيد القصدير الاستقرار الطيفي للمركبات، بينما يُحسّن أوكسيد القصدير الاستجابة البصرية المعتمدة على الطول الموجي من خلال التفاعل الانتقائي مع الضوء الساقط. تكمن الميزة الجديدة الرئيسية لهذا البحث في التكامل التآزري لأوكسيد الجرافين مع كلٍّ من أوكسيد القصدير وأوكسيد الفوسفور ضمن مصفوفة البولي أنيلين، مما يسمح بتعزيز متزامن ومتوازن للخواص الكهربائية والبصرية. يُنتج هذا التحسين متعدد الجوانب مركبات نانوية ذات تطبيقات واعدة في التقنيات المتقدمة. تشير النتائج إلى استخدامات واعدة في الأجهزة الإلكترونية البصرية، وأجهزة الاستشعار الكيميائية، والأنظمة الإلكترونية المطبوعة، مما يدعم تطوير مواد متعددة الوظائف لتقنيات الجيل القادم الذكية.

الكلمات المفتاحية: بولي انيلين، أوكسيد الجرافين، موصلية التيار المتردد، تحليل الأشعة فوق البنفسجية والمرئية ، اكاسيد المعادن.